Conflict Resolution for Wind-Optimal Aircraft Trajectories in North Atlantic Oceanic Airspace with Wind Uncertainties

Olga Rodionova and Banavar Sridhar
NASA Ames Research Center
Moffett Field, Mountain View, CA, USA

Hok K. Ng
University of California
Santa Cruz, CA, USA

Abstract—**Air traffic in the North Atlantic oceanic airspace (NAT) experiences very strong winds caused by jet streams. Flying wind-optimal trajectories increases individual flight efficiency, which is advantageous when operating in the NAT. However, as the NAT is highly congested during peak hours, a large number of potential conflicts between flights are detected for the sets of wind-optimal trajectories. Conflict resolution performed at the strategic level of flight planning can significantly reduce the airspace congestion. However, being completed far in advance, strategic planning can only use predicted environmental conditions that may significantly differ from the real conditions experienced further by aircraft. The forecast uncertainties result in uncertainties in conflict prediction, and thus, conflict resolution becomes less efficient. This work considers wind uncertainties in order to improve the robustness of conflict resolution in the NAT. First, the influence of wind uncertainties on conflict prediction is investigated. Then, conflict resolution methods accounting for wind uncertainties are proposed.**

Keywords—North Atlantic oceanic airspace, wind-optimal trajectories, conflict detection and resolution, wind uncertainties, strategic flight planning, stochastic optimization algorithm

I. INTRODUCTION

The North Atlantic oceanic airspace (NAT) joins two densely populated continents: North America and Europe. More than a thousand flights cross the NAT daily [1]. The duration of a transatlantic flight can exceed 10 hours where an aircraft can spend 3-4 hours in the NAT. Flight efficiency and environmental impact become essential issues for such long-haul flights [2]. These flights can be grouped into two major flows: eastbound, nighttime, flights from North America, and westbound, daytime, flights from Europe. The departure times for both flows in general lie within quite narrow time intervals, due to passenger demands and time zone differences [1]. As a result, the NAT is highly congested during peak hours. Moreover, it lacks sufficient surveillance (no radar coverage). Thus, assuring safety and efficiency of flight progress are the two main challenges of air traffic navigation in the NAT.

The efficiency of NAT flights is greatly affected by jet streams [3-5]. Jet streams are fast narrow predominantly eastbound air currents where the airspeed can achieve 200 kts [6]. Obviously, such strong winds should be considered during Flight Planning (FP). Eastbound flights prefer to follow the jet stream in order to benefit from strong tailwinds, while westbound flights would make efforts to avoid the jet stream [4]. Development of new generation surveillance and broadcast technologies [7], supported by ATM modernization projects, will allow each individual aircraft to plan and execute its trajectory with less restrictions [8]. Thus, each aircraft will be better able to take advantage of environmental conditions (weather, traffic, etc.) and to improve its efficiency (e.g. to minimize flight delays, fuel consumption, environmental impact, etc.) by flying optimal trajectories.

The problem of generating minimum-time paths for aircraft in strong winds was first addressed in 1930 [9]. Since then, numerous methods were proposed for computing time-optimal routes [10], fuel-optimal routes [11,12], climate-optimal routes (minimizing climate impact of aircraft emissions) [13] or cost-optimal routes (taking into account airspace charges) [14]. It was shown that by following Wind-Optimal (WO) routes, eastbound and westbound transatlantic flights could save about 7 and 10 minutes of cruising time on average respectively, while the maximum savings per flight could achieve one hour [5]. Potential fuel savings from exploiting WO routes were found to be 1-3% on average, and could be as large as 10% in some cases [12]. Thus, flying such WO routes is clearly preferable for each individual aircraft. However, when considered as an ensemble sharing the same airspace, these WO trajectories induce quite a large number of potential conflicts (violations of established separation norms) between aircraft [15], which increases ATC workload. This is due to the high flight concentration in space, within two major flows, and in time, during busy peak hours [16]. As a result, Conflict Resolution (CR) is needed in order to establish feasible flight routes and guarantee flight safety.

The Conflict Detection and Resolution (CD&R) problem has been addressed in many different ways, comprehensively overviewed in [17]. As the area of the present study is the NAT, CD&R methods for cruising phase of flights are of the greatest interest. In this frame, two types of applications can be distinguished: tactical CR, performed up to 30 minutes before a conflict is predicted for a small set of flights directly involved in this conflict; and strategic FP and CR, applied for a large set of aircraft in a particular airspace several hours before take off.

The majority of CD&R methods are developed at the tactical level, where conflicts can be resolved by changing aircraft heading, control points position, speed, flight level, or any combination of these maneuvers [18-20]. However, the subject of the present study is strategic CD&R. Several studies have already been conducted in this area [16,21-24]. The main drawback of these approaches is that the FP and CR, being performed far in advance, can only refer to the forecast wind fields available at the moment of planning. Forecast winds, however, may significantly differ from actual winds experienced by aircraft once en-route.

Meteorological forecast used for FP is provided by Numerical Weather Prediction (NWP) models [25], which incorporate all available information, obtained from radiosondes, satellite systems and automated aircraft reports [26]. NWP models, being constantly improved, nevertheless cannot exactly represent the complex nature of wind. Thus, forecast uncertainties, related to modeling are inevitable [27,28]. Uncertainties in wind forecast induce uncertainties in trajectory prediction [29,30], which turn into uncertainties in conflict prediction. As a consequence, the results of CR may become inconsistent: unpredicted conflicts may reappear in the yielded set of conflict-free trajectories when this set is evaluated against real winds.

The aim of the present study is to take into account wind uncertainties when performing strategic CR for a set of WO trajectories in the NAT. The paper is organized as follows. Section II describes the input data used in simulations, and the Conflict Detection (CD) methodology. In Section III, a wind uncertainty model is presented, and correlations between winds and conflict prediction are revealed. Finally, in Section IV, an implemented CR algorithm is described and its various modifications to account for wind uncertainties are compared. Obtained results are summarized in Section V.

II. CONFLICTS IN WIND-OPTIMAL TRAJECTORY SETS

This Section first describes the wind and flight data for WO trajectories used in the simulations of the NAT traffic. Then, a CD methodology is presented. Finally, conflict distribution is analyzed over a month with different wind conditions.

A. Wind and flight data

In the present study, 29 days of NAT traffic for July 2012 are investigated (from July 2nd to July 30th). Simulations are performed using forecast wind data and optimal trajectories for this set of winds for the 29 days. Wind data are obtained from the Global Forecasting System (GFS), a NWP model run by the National Oceanic & Atmospheric Administration (NOAA) every 6th hour. Thus, four wind forecasts are produced daily. Each such forecast is recorded in terms of u (east-west) and v (south-north) wind components in a 3-dimensional grid, covering the world airspace with 0.5-degree resolution in both longitude and latitude, and 1,000 feet resolution in altitude. An example of forecast wind on July 15th at 0000 UTC (Coordinated Universal Time format, displaying GMT time, where first two digits stand for hours and last two digits stand for minutes) at flight level FL370 (37,000 feet) is shown in Fig. 1. The jet stream current over the NAT can be clearly distinguished with high u-component and magnitude.

For each of the studied days, a set of real NAT flights is selected, and WO trajectories based on forecast are produced for these flights by solving the equations of aircraft motion in winds using the methods presented in [12]. The resolution is performed under the assumption that each aircraft maintains constant airspeed and flight level, which is credible for a cruising phase of transatlantic flights within the NAT [1]. A resulting WO trajectory is given in the form of a sequence of geographical points (longitude, latitude) recorded with one-minute interval from Origin Airport (OA) to Destination Airport (DA) (omitting takeoff and landing flight phases). It can be equally considered as a sequence of 4D-points (longitude, latitude, altitude, time).

B. Conflict detection methodology

By definition, a conflict is a violation of established separation norms. These norms are typically defined for vertical, horizontal and, in some cases, temporal separation. In the present study, only conflicts occurring within the NAT are considered. Currently, without the radar coverage, NAT traffic is restricted to follow predefined routes, named Organized Track System (OTS). The separation norms established within OTS are very large for safety consideration: 1,000 feet for vertical separation (the distance between adjacent flight levels), 60 NM for lateral separation (the distance between adjacent tracks), and from 10 to 15 minutes for temporal, in-trail, separation (for aircraft on the same track) [1]. With the upcoming innovations in surveillance and broadcast technologies, these norms could be significantly reduced [31]. In the present study, the reduced separation norms are used for
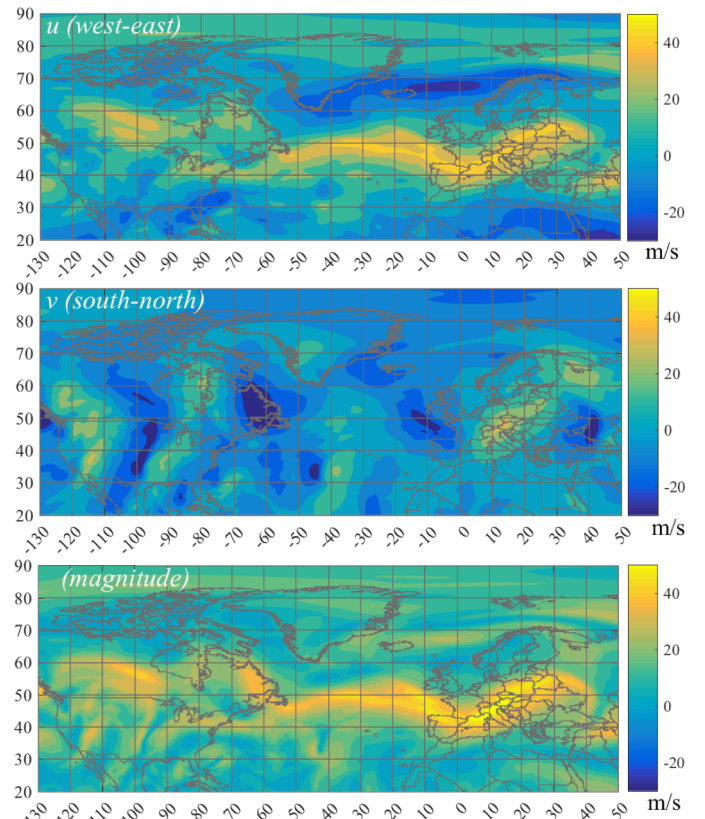

Fig.1. Forecast wind field on July 15th 2012 at 0000 UTC at FL370: u-component (top), v-component (middle), and magnitude (bottom), in m/s

CD: 1,000 feet for vertical separation, 30 NM for horizontal separation, and 3 minutes for temporal separation (a commercial aircraft cruising at the highest speed in 3 minutes would cover a distance equal to about 30 NM).

The CD method, applied in this study, was described in [21], and adapted to NAT in [15,16]. It is based on the 4-dimentional grid discretizing airspace and time, where each 4D-trajectory point is placed in an appropriate cell depending on its coordinates. The number of "point-to-point conflicts", C_t, is calculated as the number of point pairs that violate separation norms, where these pairs are taken from the same or neighbor cells of the grid. Several point-to-point conflicts involving the same aircraft trajectory pair are considered as one "trajectory-to-trajectory conflict". Thus, a pair of trajectories is in conflict, if any pair of their points is in conflict. In this study, the number of trajectory pairs in conflict is referred simply as "the number of conflicts".

Some results of the CD methodology are shown in Fig. 2. For the 29 days of July 2012, there are between 1000 and 1200 flights crossing NAT daily. These aircraft, when flying pre-computed WO trajectories, induce on average 400-600 potential conflicts under the reduced separation norms. In Fig. 3, an example of NAT traffic on July 15th is displayed. The two traffic flows can be clearly seen: eastbound flow following the jet (blue), and westbound flow (black) shifted more to the north. The detected conflicts (red) are mainly situated within these flows with high flight concentration.

C. Conflict patterns

In the first step of the research, conflict distribution over a monthly period is analyzed in order to select conflict patterns, i.e. the conflicts that repeat most often. For the 29 days of July 2012, there are 214 different OA-DA pairs present for each of the days, or, in other words, 214 similar routes were flown every day. Thus, for each day, there are about 23,000 possible
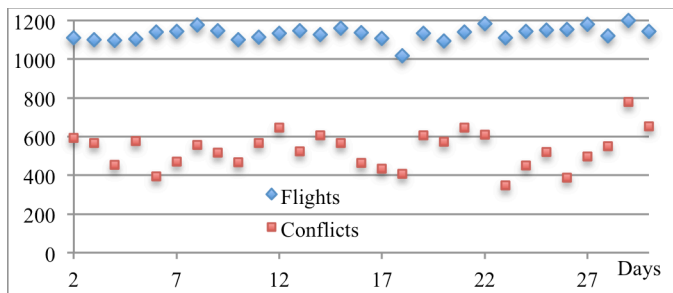

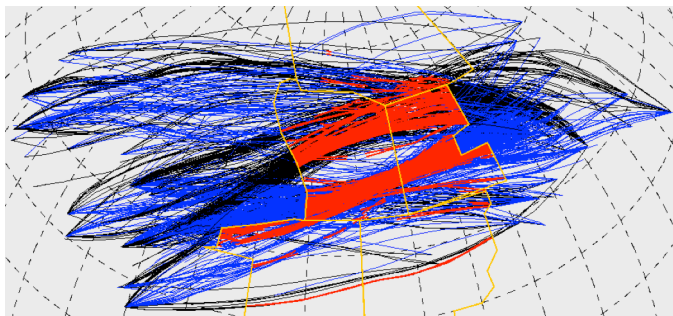Fig. 2. Number of flight (blue) and number of conflicts (red) over 29 days

Fig. 3. NAT traffic on July 15th 2012: eastbound flights (blue), westbound flights (black), conflicts (red), NAT Oceanic Control Areas (OCAs) boundaries (yellow lines)

route interactions (number of different route pairs). Among these, only 2,801 interactions generate at least one conflict in 29 days. The remaining route pairs are conflict-free, due to different flight levels, departure times and lateral spacing. Among the conflicted routes, 526 have common OA or DA. Aircraft departing from/arriving to the same airport at the same time will obviously be in conflict, and thus, no further analysis is necessary in this case.

Furthermore, among all detected conflicts, 65% occur just once, and are never repeated for the rest of the days; about 10% from the total number of conflicts are registered for more than 3 days; and less than 1% (i.e. 24 conflicts) occur for more than 9 days, and thus, could form stable conflict patterns. About 93% of conflicts within pairs of routes with different OAs and DAs happen only once per 10 days or even more rarely. For the majority of the 24 conflicts occurring for more than 9 days, both routes in a pair have the same origin or destination city (e.g. New York and London have more than one international airport). The OAs/DAs for the same city, if not the same, are still very close, and thus, the resulting routes are also very close, or even almost identical. Again, conflict nature in this case is obvious, and no analysis is necessary. As a result, there are only 3 route pairs with different origin/destination cities that induce conflicts for 9 days or more.

Consider, for example, conflicts recorded for 12 days for the routes from New York (KJFK) to London, Heathrow (EGLL), and from Boston (KBOS) to Paris, Charles de Gaulle (LFPG). Among them, there are 8 days when conflicts occur between aircraft departing between 2200 UTC on the previous day and 0000 UTC; and 9 days when conflicts occur between aircraft departing between 0200 UTC and 0300 UTC, selected for further analysis. For the route KBOS-LFPG, there is just one flight per day departing between 0200 UTC and 0300 UTC, except 2 days with no flights. The selected set of flights for 27 days is presented in Fig. 4 (top, blue). For the route KJFK-EGLL, there are several flights departing within the given time period daily. Among them, conflicted flights and flights with close departure times are selected, one per day. The resulting set of 29 flights is shown in Fig. 4 (bottom, black). As can be seen, the WO trajectories for the same airport pairs are not identical for different days.

Fig. 5 displays the conflicts (in red) detected between the routes KBOS-LFPG and KJFK-EGLL over 29 days. It can be noticed (Fig. 5, top) that the OAs and DAs for both routes are quite close, lying on the same axis, within the major eastbound traffic flow (see Fig. 3). Moreover, the structure of the recorded conflicts can be clearly distinguished: they are represented as continuous lines (Fig. 5, bottom). Such conflicts can be referred to as "continuous conflicts", which means that trajectory pairs remain in conflict for a great portion of their length. Continuous conflicts result from the fact that the two trajectories are almost identical (e.g. the two very top lines merged in one in Fig. 5, bottom) or quasi parallel separated by a small distance (e.g. the two lowest lines in Fig. 5, bottom). This is, in its turn, due to the close position of WO trajectories generated for closely situated OAs/DAs. Thus, continuous conflicts are likely to repeat from one day to another regardless of the wind. This is also a case for the majority of conflicts detected for route pairs with common OA and/or DA.

The opposite of continuous conflicts are "spot conflicts", i.e. conflicts that happen just in a single point, or a relatively small region, where the trajectories cross. An example of such conflicts is given by the intersection of routes from New York (KJFK) to Istanbul (LTBA), and from Minneapolis (KMSP) to Paris (LFGP). This pair of routes induces conflicts for 2 days only, and these conflicts occur between aircraft departing between 1600 UTC and 1700 UTC. The route KMSP-LFGP is served by just a single flight daily within the selected time period. For the route KJFK-LTBA, in general there are 2
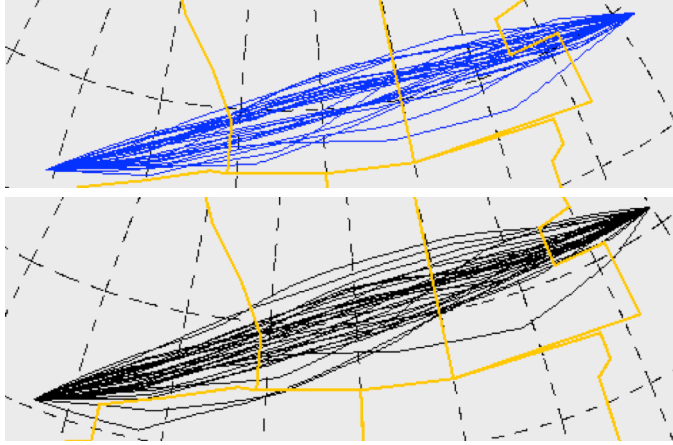

Fig. 4. Trajectories from KBOS to LFPG for 27 days (top, blue), and trajectories from KJFK to EGLL for 29 days (bottom, black)
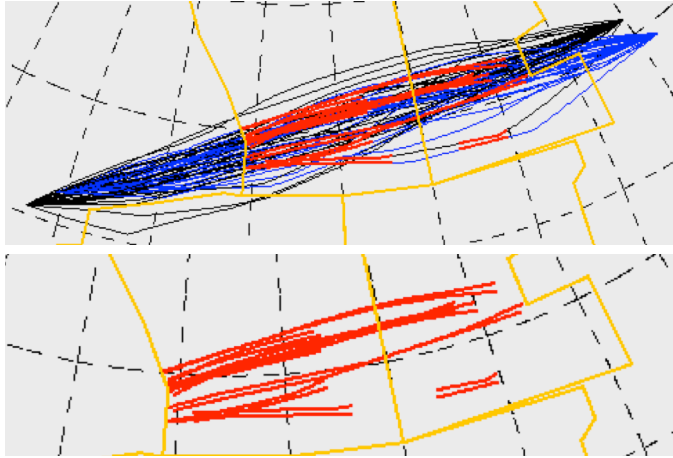

Fig. 5. Trajectories from KBOS to LFPG (blue), and from KJFK to EGLL (black) for 29 days, with conflicts (red), detected for 9 days (bottom: conflict points only)
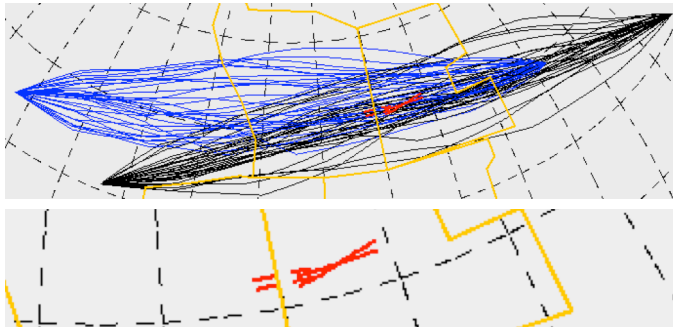

Fig. 6. Trajectories from KMSP to LFGP (blue), and from KJFK to LTBA (black) for 29 days, with conflicts (red), detected for 2 days (bottom: conflict points only)

flights per day for the same time period. Among these flights, the second ones are selected for each day, as they are more likely to induce conflicts. The resulting flights are presented in Fig. 6 (in blue for KMSP-LFGP route, and in black for KJFK-LTBA route), where the two spot conflicts detected for these sets of flights are marked with red.

The two discussed examples describe the common features of continuous and spot conflict patterns revealed for all routes being considered. Continuous conflicts depend mostly on the OA/DA positions and departure times, and do not in general depend on winds, thus, they are found to be persistent regarding wind changes. In contrast to them, spot conflicts are very sensitive to wind changes, and for majority of cases are found to be unpredictable, and would be never reproduced in different conditions.

III. CONFLICTS IN VARIABLE WIND FIELDS

In order to further investigate conflict behavior in winds, wind uncertainties related to forecast are to be considered. In this section, first different uncertainty models are discussed, and the model used in further simulations is stated. Next, the conflicts for initial sets of WO trajectories are evaluated in the wind fields with uncertainties. Finally, a correlation between variable winds and different conflict patterns is revealed.

A. Forecast wind uncertainties

Forecast errors have been a subject of numerous studies and are found to have a very complex statistical structure [32]. In many works, these errors are addressed using statistical models with Gaussian distributions, where winds are considered to be isotropic, with uncorrelated u and v components [3,33-35]. In reality, however, the NWP models do not address wind uncertainties in terms of statistical probabilities, but rather in terms of discrete scenarios, or data series. Such scenarios are produced by Ensemble Prediction Systems (EPS) [36]. Ensemble forecasts are found to represent weather uncertainties quite well [37], and are most often used when such uncertainties need to be considered in various applications [38-40]. In the present paper, similar wind scenarios are used in further simulations.

However, the wind data provided by GFS contains just one wind scenario, which was used for WO trajectories generation. Thus, the ensemble of forecast scenarios is to be modeled. For each day, 5 different wind scenarios are generated. The given scenario is referred to as "s0". It contains 4 wind field forecasts for 4 consecutive time periods. The new wind scenarios are generated by shifting the time periods to the next ("s+1", "s+2") or previous ("s-1", "s-2") day (Fig. 7). For example, for

Previous day	0000					
	0600					
	1200	s-2, 00				
	1800	s-2, 06	s-1, 00			
Current day	0000	s-2, 12	s-1, 06	s0, 00		
	0600	s-2, 18	s-1, 12	s0, 06	s+1, 00	
	1200		s-1, 18	s0, 12	s+1, 06	s+2, 00
	1800			s0, 18	s+1, 12	s+2, 06
Next day	0000				s+1, 18	s+2, 12
	0600					s+2, 18
	1200					
	1800					

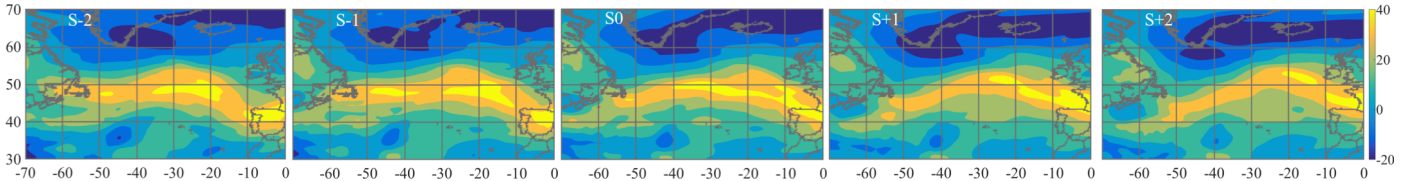Fig. 7. Modeling of 5 wind forecast scenarios

Fig. 8. Five forecast scenarios for *u* (east-west) wind component over NAT on July 15th 2012 at 0000 UTC at FL370

"s+1", the wind on the current day at 0600 UTC becomes the wind at 0000 UTC, and the wind on the next day at 0000 UTC becomes the wind at 1800 UTC on the current day, and so on. The resulting scenarios for *u*-component (most meaningful for transatlantic flights) on July 15th at 0000 UTC at FL370 are shown in Fig. 8. In addition to this, the corresponding minimum and maximum wind fields are generated for each day, by extracting minimum and maximum values over the 5 scenarios for *u* and *v* at each grid point. Fig. 9 displays such wind fields for *u* on July 15th at 0000 UTC at FL370. It is further supposed that the possible wind fluctuations remain within these minimum and maximum borders.

B. Cruising time and conflict prediction uncertainties

Uncertainties in wind forecast cause uncertainties in cruising time prediction. For example, for July 15th, an average difference between expected minimum and maximum times at NAT entry point given the same departure time (calculated based on the minimum and maximum wind fields, Fig. 9) is 10 minutes, and an average difference at NAT exit point is 21 minutes; the difference between estimated minimum and maximum total cruising times is 32 minutes on average, and reaches 1 hour in the worst case. The distribution of such differences for July 15th is shown in Fig. 10. Fig. 11 displays the mean and standard deviation values of such differences for 29 days of July. Mean values for NAT entry, NAT exit and total cruising time differences vary around 10, 20 and 30 minutes respectively, while the standard deviations for the majority of cases vary from 6 to 9 minutes.

Such large uncertainties in time prediction, in turn, induce errors in conflict prediction. Thus, the number of conflicts detected in different wind fields would be different. Fig. 12 displays the number of initial conflicts for WO trajectories over 29 days, recorded for the 5 forecast scenarios described above, as well as the number of common conflicts present for all the scenarios (cyan starts). The number of common conflicts represent on average only 70% from the total number. The remaining conflicts (from 100 to 200 for majority of days) vary from one scenario to another. However, such conflicts have equal probability to appear and disappear when the wind changes. Thus, the total number of initial conflicts does not vary a lot between scenarios, as shown in Fig. 12 (for each day, markers for scenarios from "s-2" to "s+2" are found to be almost in the same place).
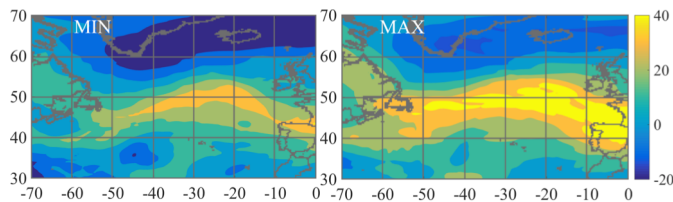

Fig. 9. Minimum (left) and maximum (right) fields for *u* (east-west) wind component over NAT on July 15th 2012 at 0000 UTC at FL370

Several examples of conflict variations in wind fields are displayed in Fig. 13, where left and right columns correspond to conflicts recorded for scenarios "s-2" and "s+2" respectively. The pair of trajectories from Brussels (EBBR) to New York (KEWR) and from Frankfurt (EDDF) to Charlotte (KCLT) induces a conflict of "continuous" type, extended for a great portion of the routes (Fig. 13, top). The conflict width is slightly reduced for "s+2" in comparison to "s-2", but in general, this conflict is barely affected by wind changes. This is the case for the majority of continuous conflicts: they remain robust under wind uncertainties. On the other hand, spot conflict variation is more noticeable. For the pair of trajectories from Amsterdam (EHAM) to Minneapolis (KMSP) and from
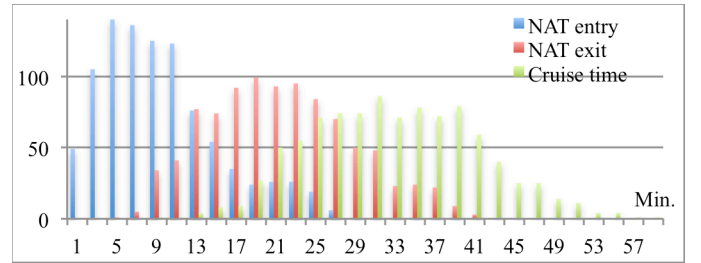

Fig. 10. Distribution of the number of flights depending on the differences (in minutes) between minimum and maximum times recorded at NAT entry, at NAT exit, and at arrival (total cruising time)
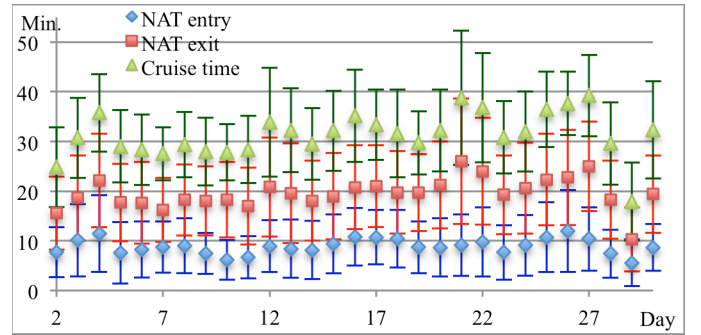

Fig. 11. Mean and standard deviation of the differences (in minutes) between minimum and maximum times recorded at NAT entry, at NAT exit, and at arrival (total cruising time) over 30 days
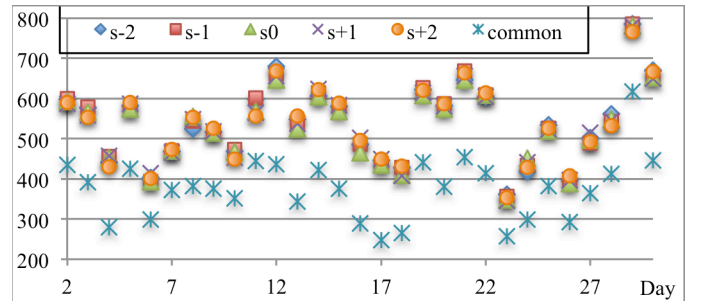

Fig. 12. Number of initial conflicts for 29 days of flights evaluated over 5 forecast wind scenarios (cyan stars: number of common conflicts, detected for all the scenarios)
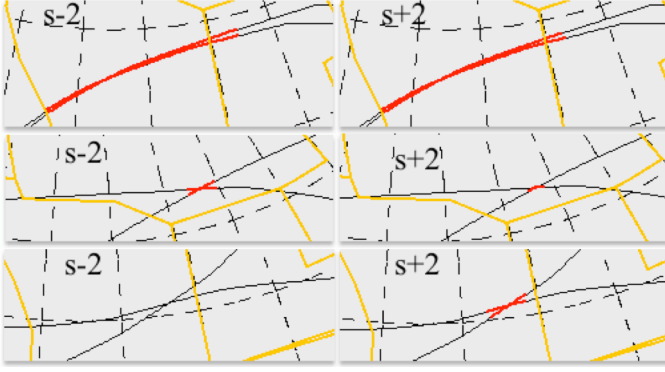
Fig. 13. Examples of conflicts recorded for different forecast wind scenarios, "s-2" (left column) and "s+2" (right column). Trajectory pairs: from EBBR to KEWR and from EDDF to KCLT (top); from EHAM to KMSP and from ESSA to KEWR (middle); and from KEWR to ENGM and from KORD to LIRF (bottom)

Fig. 14. Trajectory shape modification approach: the new trajectory (red) is obtained by shifting each point (q_i) of the initial trajectory (blue) along the normals perpendicular to the great circle (black) from origin (q_1) to destination (q_N) by the value (y_iL) defined by the cosine-like function

Stockholm (ESSA) to New York (KEWR), a spot conflict is detected for all the 5 scenarios, but its width reduces noticeably when passing from "s-2" to "s+2" (Fig. 13, middle). At the same time, trajectories from New York (KEWR) to Oslo (ENGM) and from Chicago (KORD) to Rome (LIRF) remain conflict-free for "s-2", but for "s+2", a spot conflict appears at the route intersection (Fig. 13, bottom). In general, the majority of conflicts, which appear/disappear when the wind changes, are of the "spot" type. Thus, spot conflicts are found to be much more difficult for prediction with wind uncertainties.

IV. CONFLICT RESOLUTION WITH WIND UNCERTAINTIES

This section addresses the CR problem. First, a basic CR algorithm for strategic FP is presented, and its robustness is examined with respect to changing winds. Next, several algorithm extensions intended to take wind uncertainties into account are discussed. The results of simulations are then compared, and conclusions are provided on good strategic CR.

A. Strategic conflict resolution algorithm

The CR method for strategic FP, considered in the present study, was first developed in [21], and then adapted to NAT flights following WO trajectories in the presence of winds in [15,16]. To apply this method, first, the CR problem is formulated in terms of an optimization problem. The input data for the optimization problem for a particular day of traffic are the 4 wind fields for this day (for simplicity, referred further as an ensemble, W), and a given set of N WO trajectories, where each trajectory, f ($f=1,\ldots,N$), is flown with predefined speed and flight level, and is represented as a sequence of 4D points in space and time (see Section II.A).

In order to resolve conflicts, the initial trajectory set is to be modified. In this study, two possible modification maneuvers are considered: flight delay at the departure, and modification of the trajectory geometrical shape. In the first case, a random delay, d^f, is added to the given departure time of flight f. To obtain the results reasonable from the operational point of view, a flight can be delayed by integer number of minutes, up to 30 minutes ($d^f \in \{0,1,2,\ldots,30 \text{ min}\}$). In the second case, each geographical point of the given trajectory is shifted along an arc on the Earth with the help of a cosine-like function keeping the resulting trajectory as smooth as the initial WO one
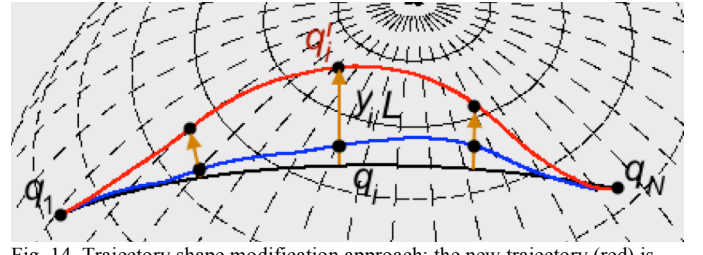
(Fig. 14). The function curvature is controlled independently for each flight f using a single real variable, b^f ($b^f \in [-1,1]$). More detail on the shape modification can be found in [16].

The values of d^f and b^f over the N flights form a vector of the optimization decision variables: $z=(d^1,b^1,\ldots,d^N,b^N)$. In the current formulation, the only constraints of the problem are the boundary constraints on the decision variables. The objective function to be minimized is given by the total number of point-to-point conflicts, C_t, induced by the set of modified trajectories corresponding to the variables z in the current wind conditions, W, (1):

$$\min_z C_t(z,W) \qquad (1)$$

As the number of conflicts, C_t, cannot be explicitly represented in terms of decision variables, z, the problem is found to be a difficult high-dimensional mixed-integer derivative-free ("black box" type) optimization problem. Thus, a stochastic metaheuristic method was implemented to tackle this problem. The method is based on the Simulated Annealing algorithm (SA), that imitates the annealing of the metal in thermodynamics, involving heating and iterative process of controlled cooling [41]. The algorithm is initialized with the current solution, z (the given set of WO trajectories), which is evaluated regarding the number of detected conflicts. Then, the neighbor solution, z^I, is generated by applying random modification maneuvers (delay or shape modification) to several trajectories. Next, this new solution is evaluated, and is accepted or rejected according to the classic SA scheme. The algorithm proceeds then to the next iteration, until the conflict-free solution ($C_t=0$) is found, or the maximum iteration number is achieved. More detail on the presented method can be found in [16,21]. It is referred further in this paper as Strategic Conflict Resolution with Simulated Annealing, SCRSA.

B. Robustness of the basic conflict resolution algorithm

By applying simultaneously departure time and trajectory shape modification maneuvers to the complete WO trajectories (from OA to DA), the SCRSA manages to resolve all the initial conflicts for all 29 days of July being simulated. More detail on such results can be found in [16]. An example of the trajectory set obtained after resolution for July 15th, when "s0" wind scenario was used for wind fields, is shown in Fig. 15. The simulation results are very advantageous when the given forecast wind is considered as the only possible wind.

However, when wind uncertainties are introduced, the neatness of the SCRSA results is compromised: undetected

conflicts reappear when the conflict-free trajectory sets yielded by SCRSA are evaluated in different wind fields. Fig. 16 demonstrates an example of conflicts for July 15th, which appear when the solution from Fig. 15 is evaluated over "s-2" scenario. Multiple red crosses corresponding to spot conflicts can be easily distinguished, while continuous conflicts are present as well. Fig. 17 displays the number of conflicts detected for the 5 wind field scenarios after the SCRSA was executed with the scenario "s0" considered as nominal wind. For this scenario, evidently, there are no conflicts, while for the shifted scenarios the number of reappeared conflicts is more or less proportional to the shift.

On average, for the scenarios "s-1" and "s+1", closest to the basic scenario "s0", the number of reappearing conflicts represents about 15% of the initial number of conflicts; while for the farthest scenarios, "s-2" and "s+2", this number represents about 20% on average, and achieves 30% in the worst cases. This means, that more than 70% of the initial conflicts are nevertheless resolved for all the scenarios for all the simulated days; and on average, the number of resolved conflicts for the shifted scenarios is 80-85%. Thus, CR for
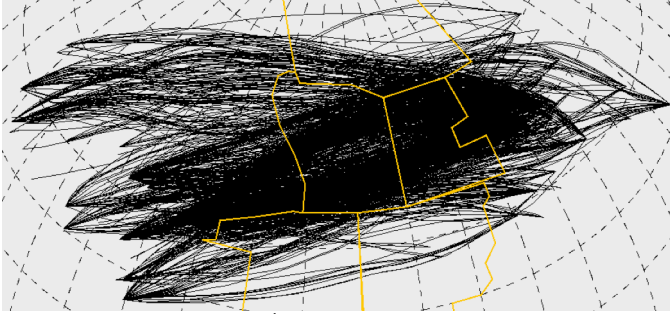

Fig. 15. NAT traffic on July 15th after conflict resolution under "s0" wind forecast scenario: no conflicts
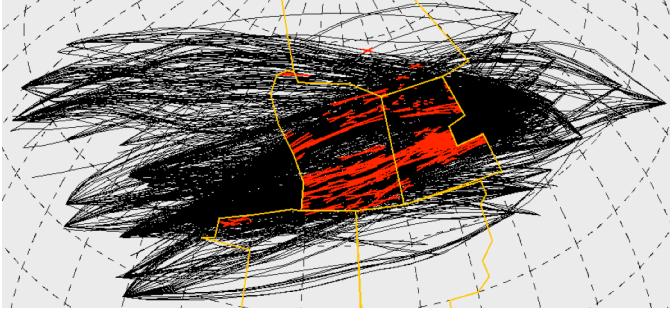

Fig. 16. NAT traffic on July 15th after conflict resolution under "s0" wind forecast scenario evaluated over "s-2" wind forecast scenario: conflicts reappear (in red)
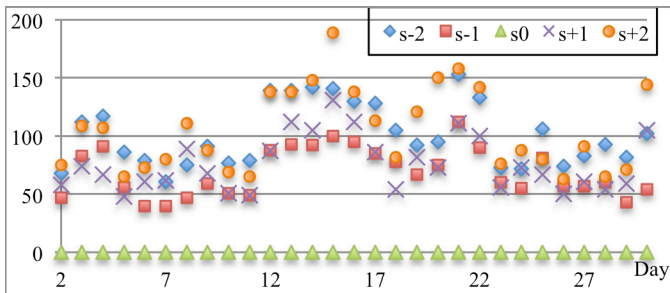

Fig. 17. Number of conflicts for 29 days after conflict resolution under "s0" wind forecast scenario evaluated over 5 wind forecast scenarios

strategic FP does make sense even if wind uncertainties are not taken into account, as the produced trajectory sets are much less conflicted than initial WO sets (Fig. 16 compared to Fig. 3), and could be treated much more easily during the tactical CR. Several ideas how the SCRSA can be modified in order to take into account wind uncertainties have been investigated. In the next section, the most reasonable ones are presented and compared.

C. Conflict resolution considering wind uncertainties

1. The first idea is, given several wind scenarios, to calculate the number of conflicts independently for each scenario and to minimize these numbers of conflicts simultaneously (2):

$$\min_z \sum_s C_t(z, W(s)), \qquad (2)$$

where $W(s)$ is the ensemble of wind fields corresponding to the scenario s (for the studied case, $s \in \{s\text{-}2, s\text{-}1, s0, s\text{+}1, s\text{+}2\}$). This solution is perfect when the wind forecast is indeed given in terms of scenarios, and when the probability that the real wind would fit one of the scenarios is high. However, this is not always the case in reality. Moreover, this method demands much more computational time: on average, N_s times more than the SCRSA, where N_s is the number of different scenarios (N_s=5 for the studied case). The method is further referred to as SCRSA/S, where "S" stands for "scenarios".

2. Next idea of SCRSA modification is to evaluate the number of conflicts in a single wind field (3) expressed as an average over all the scenarios (4):

$$\min_z C_t(z, \overline{W}), \qquad (3)$$

$$\overline{W} = \frac{1}{N_s} \sum_s W(s). \qquad (4)$$

This approach (further referred to as SCRSA/A, where "A" stands for "average") is simple and does not affect the computational time in comparison to the SCRSA. Moreover, it can be applied to any wind forecast (not obligatory based on scenarios) once the average winds are known. On the other hand, the diversity of wind uncertainties (e.g. provided by scenarios) is lost by this method.

3. Another way to incorporate such diversity is to consider minimum and maximum wind fields (6), to calculate the number of conflicts independently in these winds, and to minimize these numbers simultaneously (5):

$$\min_z C_t(z, W_{min}) + C_t(z, W_{max}), \qquad (5)$$

$$W_{min} = \min_s W(s), \quad W_{max} = \max_s W(s). \qquad (6)$$

Minimum and maximum wind conditions are more likely to be forecast in reality than exact wind scenarios, thus, this idea is feasible. Furthermore, if the final number of conflicts for the resulting solution is low (or zero) in minimum and maximum winds, it could be expected to remain low for any intermediate wind field. However, this is not guaranteed. The computational time for this method, denoted as SCRSA/M ("M" standing for "min-max"), is increased by 2 on average.

4. Ideally, the most robust solution, still being given minimum and maximum winds, is to calculate conflicts considering that an aircraft passes any of its route points not at a certain time moment but within an interval, from t_{min} to t_{max}, where t_{min} and t_{max} are calculated based on the W_{min} and W_{max} and separation norms. A route point is, thus, no longer represented as 4D point, but instead, as a 3D geographical point plus time interval. A conflict is detected between two route points, if the 3D points are on the same flight level, separated by less than 30 NM horizontally, and if the corresponding time intervals intersect. In this case, if all such conflicts are resolved for the time intervals, it is guaranteed that the resulting solution will remain conflict-free for any specific time moments taken within the intervals, and thus, for any random wind fields, contained between minimum and maximum winds. However, taking into account that the interval length is more than 10 minutes at NAT entry and more than 20 minutes at NAT exit on average (Figs. 12,13), it becomes evident, that such a robust separation is simply not possible in the dense NAT traffic conditions. Furthermore, it does not make a lot of sense, as minimum and maximum wind scenarios would never occur simultaneously.

5. A possible way to increase the robustness of conflict detection while keeping the resolution reasonable and feasible is to consider a conflict between two route points, p and q, with time intervals, $[t^p_{min}, t^p_{max}]$ and $[t^q_{min}, t^q_{max}]$, not as a integer value (1, if the intervals intersect, and 0 otherwise, as in the previous case) but as a probability, $c(p,q)$, which is defined as the ratio between the duration of the interval intersection, and the total duration of the combined interval (7):

$$c(p,q) = \frac{\max[0, \min[t^p_{max}, t^q_{max}] - \max[t^p_{min}, t^q_{min}]]}{\max[t^p_{max}, t^q_{max}] - \min[t^p_{min}, t^q_{min}]}. \quad (7)$$

Fig. 18 presents an example of how this probability is defined in the case when $t^p_{min} < t^q_{min} < t^p_{max} < t^q_{max}$. Evidently, (7) is applied only if the corresponding 3D points, p and q, are separated by less than separation norms, otherwise $c(p,q)$ is equal to 0. Thus, when the time intervals for the two points overlap significantly, these points are likely to be in conflict whichever are the real winds; and vise versa. On the other hand, when the time intervals overlap just at the borders, one could consider that this conflict would rarely occur in reality. In this case, by summing up such conflict probabilities over all neighbor pairs of trajectory point, an objective function to be minimized by the algorithm, $\widetilde{C}_t$, is obtained (8):

$$\min_z \widetilde{C}_t(z, W_{min}, W_{max}). \quad (8)$$

Here, $\widetilde{C}_t$ is no longer "a number of point-to-point conflicts", but a measure of the probability that the yielded solution will induce conflicts for any poss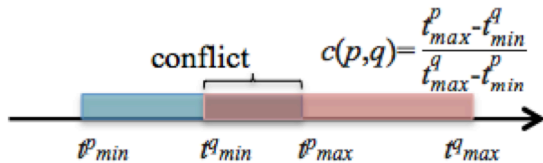ible wind field contained between minimum and maximum winds. The only drawback of the proposed method, denoted further as SCRSA/I ("I" standing for "interval") is significantly increased computational time. The efficiencies of the presented SCRSA modification methods are compared in the next section.

D. Simulation results

Four different versions of SCRSA with modifications (1, 2, 3 and 5) are compared over the 29 days of NAT traffic in July 2012. The most meaningful measure of comparison is the final number of conflicts remaining after algorithm executions. Fig. 19 displays the final number of conflicts for 29 days detected with 5 wind forecast scenarios for the solutions yielded by SCRSA/S, /A, /M, and /I (from top to bottom, respectively). Table I presents the percent of reduced conflicts compare to the initial number (Fig. 12) averaged over 29 days, for the 5 wind forecast scenarios and the 5 solutions provided by SCRSA (Fig. 17), and its 4 modifications, SCRSA/S, /A, /M, and /I (Fig. 19).

First, from Fig. 19 and Table I, it can be observed that the difference in number of conflicts between the 5 scenarios is
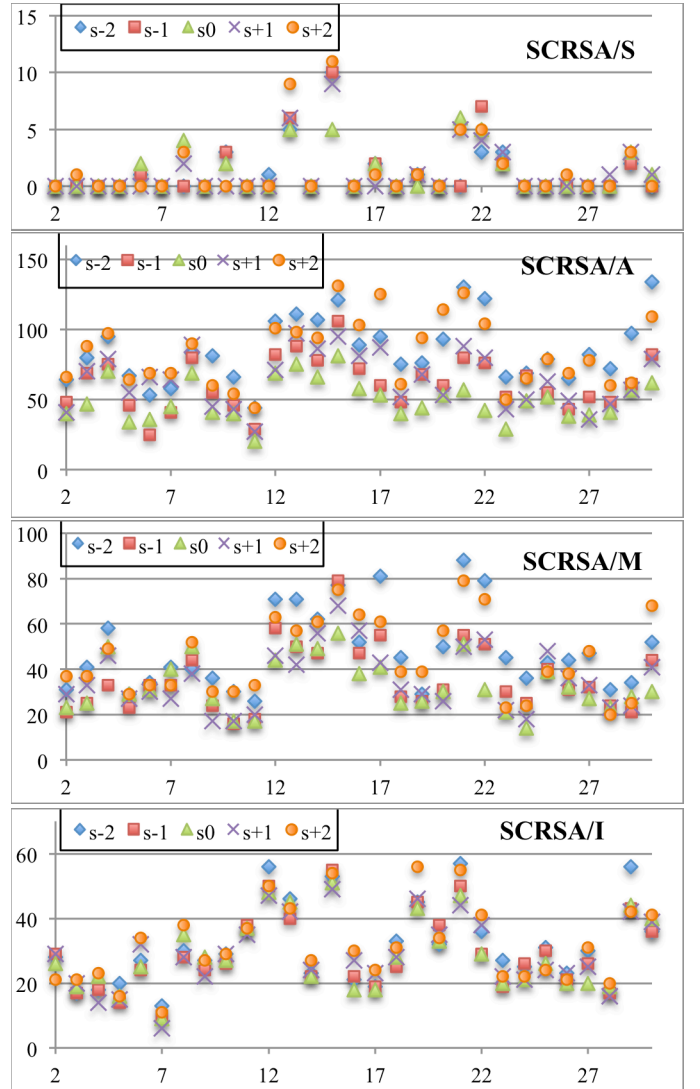

Fig. 19. Number of conflicts for 29 days evaluated over 5 wind forecast scenarios after conflict resolution with different methods

Fig. 18. Time interval when the first aircraft passes point p (blue), time interval when the second aircraft passes point q (pink), and their intersection defining the probability $c(p,q)$ that these aircraft are in conflict in these points

TABLE I.   PERCENT OF RESOLVED CONFLICT (%)

	s-2	s-1	s0	s+1	s+2
SCRSA(s0)	81.00	86.89	100	85.71	80.46
SCRSA/S	99.80	99.78	99.77	99.79	99.75
SCRSA/A	84.02	88.43	90.50	87.85	84.28
SCRSA/M	90.82	93.18	93.62	93.30	91.55
SCRSA/I	94.21	94.68	94.63	94.59	94.10

less noticeable than for the SCRSA solution (Fig. 17); especially for the SCRSA/I, where the number of detected conflicts seems to be almost equal for all the scenarios (Fig. 19, bottom). However, in general, for all the methods, this number is slightly less for "s0" and increases with the increase of the wind shift. Next, it is observed that the best results in terms of conflict reduction are yielded by the SCRSA/S (Fig. 19, top). It is quite evident, as the SCRSA/S solution is evaluated over the same wind fields that were used for resolution. It is not very correct, however, to compare this method with the rest, for which the exact information about wind scenarios is unknown.

Furthermore, algorithm SCRSA/A yields better results than SCRSA for all the scenarios except, evidently, "s0". Algorithm SCRSA/M outperforms SCRSA/A by 5% on average in terms of the number of resolved conflicts, and SCRSA/I, in its turn, outperforms SCRSA/M by 2% on average (Table I). Moreover, the solution generated by SCRSA/I is not only the one inducing the least number of conflicts for all the scenarios, but is also the one providing the most uniform conflict distribution, without obvious preference among the scenarios. It can be also noted that the greatest improvements of the results by modifications of SCRSA are achieved especially for the farthest scenarios "s-2" and "s+2". In Fig. 20, the resolution results for the 4 methods listed in Table I (except SCRSA/S) are compared for the "s+2" scenario in terms of the number of remaining conflicts over 29 days. The performance of the methods is clearly distinguished for this case.

The presented results reveal that when wind uncertainties are addressed even in a simple way, i.e. when wind variations are limited between minimum and maximum values of wind fields, CR can be noticeably improved (comparing to the CR not considering uncertainties). For the method with the highest performance, SCRSA/I, conflict reduction is estimated to be about 94-95%. Thus, only about 5% of initial conflicts are not eliminated in this case due to uncertainties. These results are very encouraging, and they prove that strategic CR does indeed make sense, as the majority of conflicts can be resolved even under quite large uncertainties in the forecast wind fields.

V.   CONCLUSION

This paper investigates strategic conflict resolution for wind-optimal trajectories in North Atlantic oceanic airspace considering wind uncertainties. Conflicts were detected within NAT under the reduced separation norms. Conflict behavior in changing wind fields was analyzed for one month of traffic. Two types of conflicts were distinguished: continuous conflicts persisting for a great portion of a flight, and spot conflicts occurring in a small area of trajectory intersection. Continuous conflicts are not significantly affected by wind changes, and are more likely to be found between the same trajectories flown on different days. Spot conflicts strongly depend on winds, and are rarely repeated from one day to another.
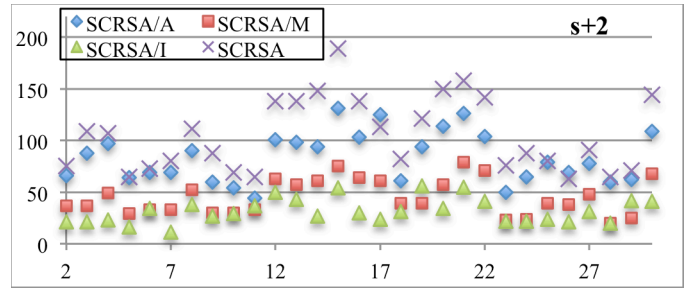

Fig. 20. Number of conflicts for 29 days evaluated over "s+2" wind forecast scenarios after conflict resolution with 4 different methods

The conflict resolution algorithm developed in previous studies for the purpose of strategic flight planning was found to be not very efficient regarding wind uncertainties, as about 20% of conflicts tend to reappear when the generated conflict-free solution is evaluated over different winds. Thus, several algorithm modifications were proposed to deal with important prediction uncertainties at the strategic level. They allow a noticeable increase to the robustness of the conflict resolution.

The best results for unknown winds were obtained when conflict probabilities were computed for intersections of time intervals calculated based on the minimum and maximum forecast wind fields. In this case, only about 5% of conflicts reappear in different wind scenarios. However, these computations are the most time-consuming: the computational time of one algorithm iteration is almost ten times greater compared to the basic algorithm, and the total execution time for one day of traffic can achieve two hours.

The method, which evaluates the trajectories in minimum and maximum winds independently, yields a compromise between the computational time (increased by about 1.7 for a single iteration, and by about 2.5 in total for the cases where a conflict-free solution is found, comparing to the basic algorithm) and the solution quality (about 8% of remaining conflicts). Finally, in the case when the most probabilistic wind scenarios are known exactly, the method evaluating trajectories over all these scenarios can be applied, which gives very good results for these particular scenarios (only 0.2% of remaining conflicts).

From the presented study, it can be concluded that the strategic conflict resolution, which is complicated because of large forecast uncertainties for the wide time horizon treated in strategic level, is nevertheless efficient when using appropriate methods. It makes it possible to obtain trajectory sets much less congested than initial wind-optimal sets, and thus, significantly reduces the workload at the tactical conflict resolution stage.

REFERENCES

[1]   NAT Doc 007, "Guidance concerning air navigation in and above the North Atlantic MNPS airspace": ICAO, 2012.

[2] N.Y. Chen, P.G. Kirschen, B. Sridhar, H.K. Ng, "Identification of flights for cost-efficient climate impact reduction", AIAA/3AF Aircraft Noise and Emissions Reduction Symposium, Atlanta, GA, USA, 2014.

[3] S. Mondoloni, "Aircraft trajectory prediction errors: Including a summary of error sources and data": Technical report, FAA/Eurocontrol, 1998.

[4] E.A. Irvine, B.J. Hoskins, K.P. Shine, R.W. Lunnon, and C. Froemming, "Characterizing North Atlantic weather patterns for climate-optimal aircraft routing", Meteorological Applications, vol. 20, pp. 80–93, 2013.

[5] B. Sridhar, K. Sheth, H.K. Ng, A.R. Morando, and J. Li, "Global simulation of aviation operations", AIAA Modeling and Simulation Technologies Conference, San Diego, CA, USA, 2016.

[6] T. Woollings, A. Hannachi, and B. Hoskins, "Variability of the North Atlantic eddy-driven jet stream", Quarterly Journal of the Royal Meteorological Society, 136, pp. 856–868, 2010.

[7] "Automatic Dependent Surveillance - Broadcast In-Trail Procedures (ADS-B ITP) operational flight evaluation: Economic benefits analysis": FAA Surveillance and Broadcast Services Report, 2015.

[8] K.J. Viets, and C.G. Ball, "Validating of future operational concept for en route air traffic control", IEEE Transactions on Intelligent Transportation Systems, vol. 2(2), pp. 63–71, 2001.

[9] E. Zermelo, "Über die Navigation in der Luft als Problem der Variationsrechnung 'On the Navigation in the Air as a Problem of the Calculus of Variations'," Jahresbericht der Deutschen Mathematiker-Vereinigung, vol. 39, pp. 44–48, 1930.

[10] M.R. Jardin, and A.E.Bryson, Jr., "Method for computing minimum-time paths in strong winds", AIAA Guidance, Navigation, and Control Conference, Toronto, ON, USA, 2010.

[11] N.K. Wickramasinghe, A. Harada, and Y. Miyazawa. "Flight trajectory optimization for an efficient air transportation system", 28th International Congress of the Aeronautical Science (ICAS), Brisbane, Australia, 2012.

[12] B. Sridhar, H.K. Ng, F. Linke, and N.Y. Chen, "Benefits analysis of wind-optimal operations for trans-atlantic flights", 14th AIAA Aviation Technology, Integration, and Operations Conference (ATIO), Atlanta, GA, USA, 2014.

[13] H.K. Ng, B. Sridhar, N.Y. Chen and J. Li, "Three-dimensional trajectory design for reducing climate impact of trans-atlantic flights", 14th AIAA Aviation Technology, Integration, and Operations Conference (ATIO), Atlanta, GA, USA, 2014.

[14] B. Sridhar, H.K. Ng, F. Linke, and N.Y. Chen, "Impact of airspace charges on transatlantic aircraft trajectories", 15th AIAA Aviation Technology, Integration, and Operations Conference (ATIO), Dallas, TX, USA, 2015.

[15] B. Sridhar, N.Y. Chen, H.K. Ng, O. Rodionova, D. Delahaye, and F. Linke, "Strategic planning of efficient oceanic flights", 11th USA/Europe ATM Research and Development Seminar, Lisbon, Portugal, 2015.

[16] O. Rodionova, D. Delahaye, B. Sridhar, and H.K. Ng, "Deconflicting wind-optimal aircraft trajectories in North Atlantic oceanic airspace", Advanced Aircraft Efficiency in a Global Air Transport System Conference (AEGATS), Paris, France, 2016.

[17] J.K. Kuchar and L.C. Yang, "A review of conflict detection and resolution modeling methods", IEEE Transactions on Intelligent Transportation Systems, vol. 1(4), pp. 179–189, 2000.

[18] N. Dougui, D. Delahaye, S. Peuchmorel, and M. Mongeau, "A light propagation model for aircraft trajectory planning", Journal of Global Optimization, vol. 56(3), pp. 873–895, 2013.

[19] D. Delahaye, C. Peyronne, M. Mongeau, and S. Peuchmorel, "Aircraft conflict resolution by genetic algorithm and B-spline approximation", 2nd ENRI International Workshop on ATM/CNS, pp. 71–78, 2011.

[20] M.A. Christodoulou, and S.G. Kodaxakis, "Automatic commercial aircraft collision avoidance in free flight: The three-dimentional problem", IEEE Transactions on Intelligent Transportation Systems, vol. 7(2), pp. 242–249, 2006.

[21] S. Chaimatanan, D. Delahaye, and M. Mongeau, "A hybrid metaheuristic optimization algorithm for strategic planning of 4D aircraft trajectories at the continental scale", IEEE Computational Intelligence Magazine, vol. 9(4), pp. 46–61, 2014.

[22] M.R. Jardin, "Real-time conflict-free trajectory optimization", 5th USA/Europe ATM Research and Development Seminar, Budapest, Hungary, 2003.

[23] S. Grabbe, B. Sridhar, and A. Mukherjee, "Scheduling wind-optimal Central East Pacific flights", Air Traffic Control Quarterly, vol. 16(3), pp. 187–210, 2008.

[24] B. Girardet, "Trafic aerien: determination optimale et globale des trajectoires d'avion en presence de vent 'Air traffic: optimal and global determination of aircraft trajectories in the presence of wind',": PhD thesis, General Mathematics, Toulouse INSA, 2014.

[25] E. Kalnay, M. Kanamitsu, and W.E. Baker, "Global Numerical Weather prediction at the National Meteorological Center", Bulletin American Meteorological Society, vol. 71(10), pp. 1410-1428, 1990.

[26] W.R. Moninger, R.D. Mamrosh, and P.M. Pauley, "Automated meteorological reports from commercial aircraft", Bulletin American Meteorological Society, vol. 84, pp. 203–216, 2003.

[27] B.E. Schwartz, S.G. Benjamin, S.M. Green, and M.R. Jardin, "Accuracy of RUC-1 and RUC-2 wind and aircraft trajectory forecast by comparison with ACARS observations", Weather and Forecasting, vol. 15, pp. 313–326, 2000.

[28] E. Robert, and D. De Smedt, "Comparison of operational wind forecasts with recorded flight data", 10th USA/Europe ATM Research and Development Seminar, Chicago, IL, USA, 2013.

[29] A.G. Lee, S.S. Weygandt, B. Schwartz, and J.R. Murphy, "Performance of trajectory models with wind uncertainties", AIAA Modeling and Simulation Technologies Conference, Chicago, IL, USA, 2009.

[30] C.P. Tino, L. Ren, and J.-P.B. Clarke, "Wind forecast error and trajectory prediction for en-route scheduling", AIAA Guidance, Navigation, and Control Conference, Chicago, IL, USA, 2009.

[31] A. Williams, and I. Greenfeld, "Benefits assessment of reduced separations in North Atlantic Organized Track System", 6th AIAA Aviation, Technology, Integration, and Operations Conference (ATIO), Wichita, KS, USA, 2006.

[32] A. Hollingsworth, and P. Lonnberg, "The statistical structure of shortrange forecast errors as determined from radiosonde data. Part I: The wind field", Tellus, vol. 38A(2), pp. 111–136, 1986.

[33] I. Lymperopoulos, G. Chaloulos, and J. Lygeros, "An advanced particle filtering algorithm for improving conflict detection in Air Traffic Control", International Conference on Research in Air Transportation (ICRAT), Budapest, Hungary, 2010.

[34] A.H. Monahan, "The Gaussian statistical predictability of wind speeds", Journal of Climate, vol. 26, pp. 5563-5577, 2013.

[35] I.R. Oliveira, R. Quachio, and P.S. Cugnasca, "Improving computation of simulated wind-prediction error for air traffic applications", Journal of Aerospace Information Systems, vol. 11(7), pp. 423-432, 2014.

[36] "Guidelines on Ensemble Prediction Systems and Forecasting": World Meteorological Organization, 2012.

[37] T. Gneiting, and A.E. Raftery, "Weather forecasting with ensemble methods," Atmospheric Science, vol. 310, pp. 248-249, 2005.

[38] T. N. Palmer, "The economic value of ensemble forecasts as a tool for risk assessment: From days to decades," Quarterly Journal of the Royal Meteorological Society, vol. 128(581), pp. 747–774, 2002.

[39] J.M. Sloughter, T. Gneiting, and A.E. Raftery, "Probabilistic wind speed forecasting using ensembles and Bayesian model averaging", Journal of the American Statistical Association, vol. 105(489), pp. 25-35, 2010.

[40] D. Rivas, R. Vazquez, and A. Franco, "Stochastic prediction of cruising fuel load considering ensemble wind forecast", Advanced Aircraft Efficiency in a Global Air Transport System Conference (AEGATS), Paris, France, 2016.

[41] S. Kirkpatrick, C.D. Gelatt, and M.P.G. Vecchi, M.P.G. "Optimization by Simulated Annealing", Science, vol. 220, pp. 671–680, 1983.